

UC San Diego

UC San Diego Previously Published Works

Title

A monoclonal antibody to assess oxidized cholesteryl esters associated with apoAI and apoB-100 lipoproteins in human plasma 1 [S]

Permalink

<https://escholarship.org/uc/item/7qj81985>

Journal

Journal of Lipid Research, 60(2)

ISSN

0022-2275

Authors

Gonen, Ayelet

Choi, Soo-Ho

Miu, Phuong

et al.

Publication Date

2019-02-01

DOI

10.1194/jlr.d090852

Copyright Information

This work is made available under the terms of a Creative Commons Attribution License, available at <https://creativecommons.org/licenses/by/4.0/>

Peer reviewed



A monoclonal antibody to assess oxidized cholesteryl esters associated with apoAI and apoB-100 lipoproteins in human plasma¹

Ayelet Gonen,* Soo-Ho Choi,* Phuong Miu,* Colin Agatisa-Boyle,* Daniel Acks,* Angela M. Taylor,[†] Coleen A. McNamara,[†] Sotirios Tsimikas,* Joseph L. Witztum,* and Yury I. Miller^{2,*}

Department of Medicine,* University of California, San Diego, La Jolla, CA 92093; and Cardiovascular Research Center,[†] Department of Medicine, University of Virginia, Charlottesville, VA 22908

Abstract Atherosclerosis is associated with increased lipid peroxidation, leading to generation of multiple oxidation-specific epitopes (OSEs), contributing to the pathogenesis of atherosclerosis and its clinical manifestation. Oxidized cholesteryl esters (OxCEs) are a major class of OSEs found in human plasma and atherosclerotic tissue. To evaluate OxCEs as a candidate biomarker, we generated a novel mouse monoclonal Ab (mAb) specific to an OxCE modification of proteins. The mAb AG23 (IgG1) was raised in C57BL6 mice immunized with OxCE-modified keyhole limpet hemocyanin, and hybridomas were screened against OxCE-modified BSA. This method ensures mAb specificity to the OxCE modification, independent of a carrier protein. AG23 specifically stained human carotid artery atherosclerotic lesions. An ELISA method, with AG23 as a capture and either anti-apoAI or anti-apoB-100 as the detection Abs, was developed to assay apoAI and apoB-100 lipoproteins that have one or more OxCE epitopes. OxCE-apoA or OxCE-apoB did not correlate with the well-established oxidized phospholipid-apoB biomarker. In a cohort of subjects treated with atorvastatin, OxCE-apoA was significantly lower than in the placebo group, independent of the apoAI levels. **These results suggest the potential diagnostic utility of a new biomarker assay to measure OxCE-modified lipoproteins in patients with CVD.**—Gonen, A., S-H. Choi, P. Miu, C. Agatisa-Boyle, D. Acks, A. M. Taylor, C. A. McNamara, S. Tsimikas, J. L. Witztum, and Y. I. Miller. **A monoclonal antibody to assess oxidized cholesteryl esters associated with apoAI and apoB-100 lipoproteins in human plasma.** *J. Lipid Res.* 2019. 60: 436–445.

Supplementary key words apolipoprotein AI • apolipoprotein B-100 • biomarker • oxidation-specific epitope

This study was supported by National Institutes of Health Grants HL136275 (Y.I.M., J.L.W., S.T., A.M.T., and C.A.M.) and HL088093 (J.L.W., Y.I.M., and S.T.). National Institute of Neurological Disorders and Stroke Grant P30 NS047101 supports the University of California, San Diego School of Medicine Microscopy and Histology Core. The content is solely the responsibility of the authors and does not necessarily represent the official views of the National Institutes of Health.

Manuscript received 2 November 2018 and in revised form 15 December 2018.

Published, JLR Papers in Press, December 18, 2018
DOI <https://doi.org/10.1194/jlr.D090852>

The concept of sterile inflammation induced by host-derived damage-associated molecular patterns (DAMPs) helps to explain the inflammatory mechanisms of many chronic diseases. It is now well-documented that DAMPs share structural motifs with microbial pathogen-associated molecular patterns and activate innate immune pattern-recognition receptors (1). While these responses may provide initial benefits, the ensuing inflammatory responses may be harmful if unconstrained and prolonged, such as occurs in atherosclerosis, a life-long chronic inflammation of medium/large arteries leading to CVD.

Oxidized cholesteryl esters (OxCEs) are the DAMPs arising during the development of atherosclerosis (1–4). We have demonstrated that cholesterol binds to MD-2 (5), a ligand-binding coreceptor for the prototypic pattern-recognition receptor, toll-like receptor-4 (TLR4). MD-2 has a hydrophobic pocket and, remarkably, shares a significant structural homology with Niemann-Pick disease type C2, a lysosomal cholesterol-binding protein (6). Further, cholesterol esterified to an oxidized polyunsaturated fatty acyl chain, i.e., OxCE, when bound to TLR4/MD-2, induces TLR4 dimerization and activates inflammatory responses in macrophages (2). Importantly, specific OxCE molecules first identified in test-tube oxidation reactions are also found in cellular systems, in vascular lesions of experimental animals, and in plasma and atherosclerotic plaques

Abbreviations: AP, alkaline phosphatase; CuOxLDL, copper-oxidized LDL; DAMP, damage-associated molecular pattern; G6A, GDGDGA peptide; G6K, GDGDGK peptide; HAT, hypoxanthine-aminopterin-thymidine; HDL-C, HDL cholesterol; KLH, keyhole limpet hemocyanin; LDL-C, LDL cholesterol; 12/15LO, 12/15-lipoxygenase (gene name *Alox15*); Lp(a), lipoprotein (a); mAb, monoclonal Ab; MDA, malondialdehyde; OSE, oxidation-specific epitope; OxCE, oxidized cholesteryl ester; OxPL, oxidized phospholipid; TC, total cholesterol; TLR4, toll-like receptor-4.

¹Guest editor for this article was Alan M. Fogelman, David Geffen School of Medicine at UCLA, Los Angeles, CA.

²To whom correspondence should be addressed.

e-mail: yumiller@ucsd.edu

S The online version of this article (available at <http://www.jlr.org>) contains a supplement.

Copyright © 2019 Gonen et al. Published under exclusive license by The American Society for Biochemistry and Molecular Biology, Inc.

This article is available online at <http://www.jlr.org>

isolated from human CVD patients (3, 7–11). For example, cholesteryl arachidonate and cholesteryl linoleate oxidation products are detected in human plasma from CVD patients and in human atherosclerotic lesions (2, 3, 11), as well as in experimental studies with hypercholesterolemic mice and zebrafish (12, 13). Human atherosclerotic lesions contain OxCE not only in a free lipid form but also as covalent adducts to proteins (14). Based on these findings, we suggest that OxCE is a major DAMP arising in hypercholesterolemic animals and human subjects, which contributes to vascular inflammation and atherogenesis (4, 15).

In this study, we examined whether immunological detection of OxCE epitopes in plasma may have diagnostic value and serve as a new biomarker. We developed the monoclonal Ab (mAb) AG23 that recognizes OxCE covalent adducts irrespective of the modified protein. AG23 specifically stained atherosclerotic lesions in human carotid endarterectomy specimens. AG23 was used in conjunction with Abs targeting apoAI or apoB-100 to measure OxCE associated with apoAI- or apoB-100-containing lipoproteins in human plasma. This OxCE assay demonstrated that, in a cohort of subjects treated with atorvastatin, there was a significant reduction in OxCE-containing apoAI lipoproteins, not associated with changes in apoAI levels.

MATERIALS AND METHODS

Human plasma and tissue samples

Human plasma, used for LDL isolation, was obtained from healthy volunteers who provided written informed consent according to a protocol approved by the University of California, San Diego Human Research Protection Program. Human blood samples were also obtained from two previously published studies, the “UVA cohort” (2) and the “PROXI cohort” (16). Human carotid endarterectomy specimens were obtained from patients undergoing carotid endarterectomy with a protocol approved by the University of California, San Diego Human Research Protection Program.

Animals

All animal experiments were conducted according to protocols approved by the Institutional Animal Care and Use Committee of the University of California, San Diego. Mice were housed up to 5 per standard cage at room temperature and maintained on a 12:12 h light:dark cycle, with lights on at 0700. Both food and water were available ad libitum. Wild-type C57BL/6 mice were initially purchased from Jackson Laboratory (Bar Harbor, ME) and bred in-house.

Antigen preparation

The procedures for preparing OxCE-modified keyhole limpet hemocyanin (KLH) and BSA were identical. To prepare the OxCE-BSA antigen, cholesteryl arachidonate (Nu-Check, Waterville, MN) was oxidized as previously described (2) to produce OxCE. One milligram of OxCE dissolved in hexane was dried under argon in a glass tube, solubilized with 2.5 ml of 2.5 mg/ml BSA (Sigma) in PBS, and incubated for 1 h at 37°C with gentle agitation. After 1 h, this reaction mixture was added to an additional 1 mg of oxidized cholesteryl arachidonate dried in a separate glass tube, incubated, and the procedure was repeated one more time. This step-wise modification of the BSA with OxCE was used to prevent protein precipitation upon contact with a large

amount of lipid. At the end of the last incubation, 25 μ l of freshly prepared 30 mg/ml NaBH_3CN in PBS were added to the tube and incubated overnight at 37°C. The solution was filtered through a 0.45 μ m filter, dialyzed against PBS to remove unreacted NaBH_3CN , and sterile filtered again. The OxCE-BSA was aliquoted and frozen at -80°C . The peptide, biotin-GDGDGK (G6K; from Biomatik, Wilmington, DE), was modified with OxCE at a 1:1 molar ratio, using the same protocol as for OxCE-BSA. The biotin-GDGDGA (G6A) peptide in which the C-terminal Lys was replaced with Ala, served as a negative control. Modified LDL antigens were prepared as described in detail previously (17).

Immunization, hybridoma, and screening

The protocol for generating OxCE-specific mAbs was modified from an earlier work in our laboratory (18). Briefly, four male C57BL/6 mice (age 8–10 weeks) were immunized three times with OxCE-KLH emulsified 1:1 in incomplete Freund’s adjuvant for a primary immunization and two boosts at 2 week intervals, as illustrated in Fig. 1A. A week after the second boost, mice were bled, and IgG titers were measured by ELISA to assess direct binding to the plated antigens, OxCE-KLH and OxCE-BSA, as described in detail below. The two mice with the highest titers received an intravenous recall-boost with the antigen in PBS. Three days later, the mice were euthanized, and splenocytes were collected and fused with myeloma cells (X36Ag8.653) using a ClonaCell™-HY hybridoma kit (Stemcell Technologies, Cambridge, MA). The fused cells were resuspended in semi-solid hypoxanthine-aminopterin-thymidine (HAT) hybridoma selection medium. Two weeks later, visible colonies were transferred to ClonaCell®-HY growth medium (DMEM, preselected serum, hypoxanthine-thymidine, gentamycin, and supplements). To select OxCE-specific but not KLH-specific colonies, media supernatants from hybridoma cells were screened by ELISA against OxCE-BSA, using an anti-mouse IgG detection Ab (Sigma-Aldrich, St. Louis, MO). Selected clones were subcloned by limiting dilution in semi-solid gel, without HAT, and retested by ELISA for binding to OxCE-BSA to ensure monoclonality. The selected colony (AG23) was expanded by BioXCell (West Lebanon, NH) in tissue culture in a stirred tank fermentation with Hybridoma-SFM medium supplemented with 1% Fetal Clone 3 (Life Technologies, Carlsbad, CA) and purified with chromatography over Protein A/G resin. The AG23 heavy and light chains were sequenced by Creative Biolabs (Shirley, NY).

Mouse atherosclerosis study

Ldlr^{-/-} mice were initially purchased from Jackson Laboratory and bred in-house for experiments. *Alox15*^{-/-} mice (19) were a gift from Dr. Colin Funk and were crossbred in-house with *Ldlr*^{-/-} mice. Male mice, starting at age 8 weeks, were fed a high-cholesterol normal-fat diet (Teklad TD 97131) containing 1% cholesterol for 16 weeks. Plasma total cholesterol (TC) was measured using automated enzymatic assays (Roche Diagnostics, Indianapolis, IN). Atherosclerosis was assessed as previously described (20). Briefly, aortic root atherosclerosis was quantified by cutting cross-sections starting from the aortic origin until the last leaflet. Sections were stained with a modified Van Gieson stain and lesion area was quantified via computer-assisted image analysis (Image-Pro, Media-Cybernetics, Rockville, MD).

Western blot

BSA or OxCE-BSA (0.5 μ g/well) was subjected to gel electrophoresis and immunoblot as described (21). Briefly, samples were loaded and run on a 4–12% Bis-Tris gel (Life Technologies). Gels were incubated with Coomassie Blue for 1 h or transferred to a PVDF membrane (Life Technologies). The membranes were incubated with primary Abs (1 μ g/ml in 1% BSA-TBST) overnight at

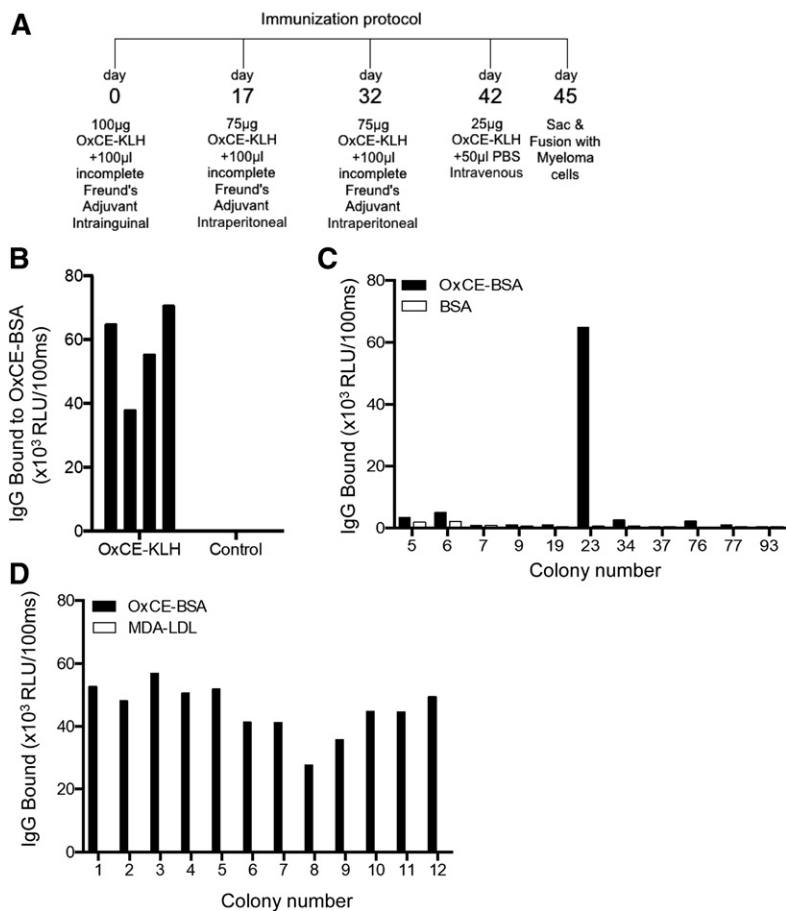


Fig. 1. Generation of OxCE-specific mAb. A: Immunization protocol. B: Following the second boost (day 40), mice were bled and 1:100 plasma samples were tested by ELISA using OxCE-BSA as an antigen. The graph represents the mean of duplicate measurements from four immunized mice and four control (nonimmunized) mice. C: Ninety-six hybridoma colonies were collected, expanded, and screened in ELISA against 5 µg/ml OxCE-BSA and BSA. The graph shows a representative result of multiple screening rounds. The positive colony #23 was retested 10 times and designated AG23. D: To ensure monoclonality, AG23 was subjected to single cell dilution using semi-solid gel without HAT. Twenty-four colonies were collected and expanded. The media were tested two times by ELISA using 5 µg/ml OxCE-BSA and MDA-LDL. The graph shows 12 representative colonies (in technical triplicates).

4°C, followed by incubation with secondary Abs conjugated with HRP for 1 h at room temperature and by detection with a Super Signal West Dura substrate (Thermo Fisher Scientific, Waltham, MA) and an OptiChem HR imaging system (UVP, Upland, CA).

ELISA with direct antigen plating

mAb binding to an array of epitopes was measured by chemiluminescent ELISA as previously described (17). In brief, wells were coated with antigens at 5 µg/ml in PBS overnight at 4°C. Following blocking with 1% BSA-TBS, hybridoma supernatant (undiluted) or purified mAb was added and incubated for 90 min at room temperature. Bound Abs were detected using an anti-mouse IgG-alkaline phosphatase (AP) conjugate (Sigma-Aldrich), a Lumi-Phos 530 substrate (Lumigen, Southfield, MI), and a Dynex luminometer (Dynex Technologies, Chantilly, VA). Ab binding was expressed as relative light units detected over 100 ms (RLU/100 ms).

Peptide-based ELISA

Biotinylated short peptides, G6A-OH, G6K-OH (non-modified), or G6K-OxCE (modified with OxCE), were immobilized to streptavidin precoated plates (Eagle Biosciences, Amherst, NH) at 10 µg/ml in PBS overnight at 4°C. After washing with PBS, AG23 was added at 1 µg/ml in 1% BSA-TBS and incubated at room temperature for 90 min. The remaining ELISA was completed as described above.

Competition ELISA

A fixed and limiting concentration of AG23 was preincubated overnight in the absence or presence of increasing concentrations of various competitors. Immune complexes were pelleted by a

45 min spin at 11,000 rpm, and supernatants were used in an ELISA as described above. Concentration of plated antigens was 5 µg/ml. Results were expressed as B/B₀ as previously described (17).

Cholesterol esterase reaction

An ELISA plate was coated with OxCE-BSA (1.25 µg/well) in PBS overnight at 4°C. After washing off unbound antigen, cholesterol esterase (MP Biomedicals, Santa Ana, CA) was added at 10 u/well in PBS and incubated for 3 h at 37°C. The solution was gently collected from the wells and analyzed for free cholesterol using a kit from BioVision (Milpitas, CA). The wells were then washed and used in the AG23 binding assay as described earlier.

Immunohistochemistry

Paraffin embedded tissue was cut into 7 µm thick sections and mounted on charged slides. The sections were deparaffinized with HistoClear, rehydrated through graded ethanol, and blocked with 5% normal goat serum/1% BSA/TBS for 30 min at room temperature. AG23 (0.1 µg/ml) was preincubated overnight at 4°C in the absence and presence of 5, 15, or 45 µg/ml of OxCE-BSA. Immune complexes were pelleted as above, and the supernatant was used to stain sections in a humidified chamber at 4°C overnight. Sections were then incubated with an anti-mouse IgG-AP (Sigma A3438) diluted with blocking buffer at 1:50 for 30 min at room temperature, and then visualized with Vector Red substrate (Vector SK-5100). Sections were counterstained with hematoxylin for 30 s, dehydrated through graded ethanol, cleared with HistoClear, and coverslipped using HistoMount. Immunostaining of consecutive sections in the absence of primary Abs was used as a negative control. Images were captured with Hamamatsu Nanozoomer 2.0HT slide scanner with a 20× lens.

Biomarker ELISA assays

To detect OxCE in human plasma, three sandwich ELISA protocols were tested. In protocol 1, plates were coated with 5 µg/ml of MB47, a mouse monoclonal specific for human apoB-100 (22), or with a sheep anti-human apoAI polyclonal Ab (Binding Site, Birmingham, UK) overnight at 4°C, followed by blocking with 1% BSA-TBS for 30 min at room temperature. Plasma samples (1:50) were added and incubated at room temperature for 90 min, followed by 0.1 µg/ml biotin-labeled anti-OxCE AG23 detection Ab, streptavidin-AP, and Lumi-Phos 530. In protocol 2, plates were coated with 5 µg/ml AG23, blocked, incubated with 1:50 plasma samples, followed by 0.05 µg/ml goat anti-human apoB-100 polyclonal Ab or 0.1 µg/ml goat anti-human apoAI polyclonal Ab (both from Academy BioMed, Houston, TX), streptavidin-AP, and Lumi-Phos 530. In protocol 3, plates were coated with 5 µg/ml unconjugated AG23 and detected with 0.1 µg/ml biotinylated AG23. We dubbed this assay as “total OxCE,” in quotation marks because it detects OxCE irrespective of the lipoprotein or protein carrier, but only if more than one AG23-accessible OxCE epitope is present.

Statistics

Graphs represent mean ± standard error as described in figure legends. Results were analyzed using Spearman correlation analysis, *t*-test (for two groups), or one-way ANOVA (for more than two groups), as provided in GraphPad Prism (GraphPad Software, San Diego, CA), and the differences with *P* < 0.05 were considered statistically significant.

RESULTS

Generation and characterization of OxCE mAb

Four mice were immunized with OxCE-KLH and screened for Ab production by binding to OxCE-BSA (Fig. 1B). Hybridomas were generated from the spleens of the two mice with the highest IgG titers and supernatants screened for IgG binding to OxCE-BSA. Clone 23 was selected for its robust IgG binding to OxCE-BSA, but not BSA (Fig. 1C). To ensure the monoclonality of the Ab, it was subjected to a single cell dilution, and all daughter clones were positive for OxCE-BSA binding (Fig. 1D). The Ab, dubbed AG23, was sequenced (supplemental Fig. S1), expanded, and purified by contract research organizations as detailed in the Materials and Methods.

The AG23 Ab stained OxCE-BSA, but not BSA, on a Western blot, while a control nonspecific IgG1 stained neither (Fig. 2A). AG23 binding to two other common oxidation-specific epitopes (OSEs), malondialdehyde (MDA)-modified LDL and oxidized phospholipid (OxPL) enriched in copper-oxidized LDL (CuOxLDL), was negligible (Fig. 2B). OxCE-KLH, but not KLH, competed with OxCE-BSA for AG23 binding (Fig. 2C), validating the specificity of the Ab to the OxCE epitope irrespective of the carrier protein. To further confirm the specificity of AG23 to the OxCE covalent modification of a protein, we modified the G6K peptide with OxCE, using the protocol utilized for the OxCE-BSA and OxCE-KLH modifications, and observed a robust AG23 binding to G6K-OxCE, but not unmodified G6K-OH (Fig. 2D). The OxCE modification procedure for the G6A peptide, in which alanine replaces the C-terminal

lysine, was not expected to result in a covalent bond between OxCE and the peptide, and indeed AG23 did not bind to the G6A/OxCE reaction product (Fig. 2D). In a cross-competition assay, both OxCE-BSA and G6K-OxCE competed with each other for AG23 binding in a dose-dependent manner (Fig. 2E, F).

Incubation of OxCE-BSA with cholesterol esterase released free cholesterol, confirming hydrolysis of the ester bond in the OxCE epitope, and nullified AG23 binding to the OxCE-BSA from which cholesteryl was cleaved off (Fig. 2G). This result suggests that the cholesterol moiety is part of the epitope recognized by AG23 or that it was necessary for the correct configuration of the AG23 epitope to be recognized.

Because OxCE products were detected in human atherosclerotic lesions using lipid extraction and mass spectrometry techniques (3, 8–11), we tested to determine whether AG23 could detect OxCE in human lesions using immunohistochemistry. AG23 specifically stained sections of human carotid artery atherosclerotic lesions, and OxCE-BSA preincubated with AG23 competed with the tissue immunostaining in a dose-dependent manner (Fig. 3). These results suggest that AG23 detects OxCE epitopes arising during the development of human atherosclerosis.

In an animal study, we compared OxCE levels in plasma from *Ldlr*^{-/-} and *Alox15*^{-/-} *Ldlr*^{-/-} mice fed a high-cholesterol diet. The enzyme 12/15-lipoxygenase (12/15LO; gene name *Alox15*) has been implicated as a major causative factor in lipoprotein oxidation *in vivo* (23, 24), with CE being a preferential substrate for the 12/15LO activity (25, 26). At the end of high-cholesterol diet feeding, levels of TC were not different (Fig. 4A), but the levels of OxCE were significantly lower in the plasma of *Alox15*^{-/-} *Ldlr*^{-/-} mice compared with that of *Ldlr*^{-/-} mice (Fig. 4B). The lower plasma levels of OxCE corresponded with reduced size of atherosclerotic lesions in *Alox15*^{-/-} *Ldlr*^{-/-} mice (Fig. 4C), the latter in agreement with earlier reports (27).

OxCE biomarker immunoassay

We next sought to determine whether we could detect OxCE epitopes in human LDL captured on microtiter wells using the apoB-100-specific Ab, MB-47. LDL was captured from human plasma samples on MB-47-coated wells, and AG23 was added to detect OxCE epitopes on the LDL [Fig. 5A (A1)]. However, detection levels were low for most of the samples (Fig. 5B, empty bars), despite the efforts to optimize antigen/Ab concentrations and conditions of assay. Then, we flipped the sandwich and used AG23 as a capture Ab and a biotinylated anti-apoB-100 as the detection Ab [Fig. 5A (A2)]. In this format, signal was robust, with a wide range of levels detected in different human plasma samples (Fig. 5B, blue bars). However, in this format, different amounts of LDL could be captured per well depending on the LDL concentration, and/or captured LDL particles may have one or more OxCE epitopes.

To detect OxCE associated with apoAI lipoproteins, we kept the AG23 capture format, but replaced the biotinylated apoB-100 Ab with a biotinylated anti-apoAI Ab. In this formulation, we detected robust signal for OxCE-apoA,

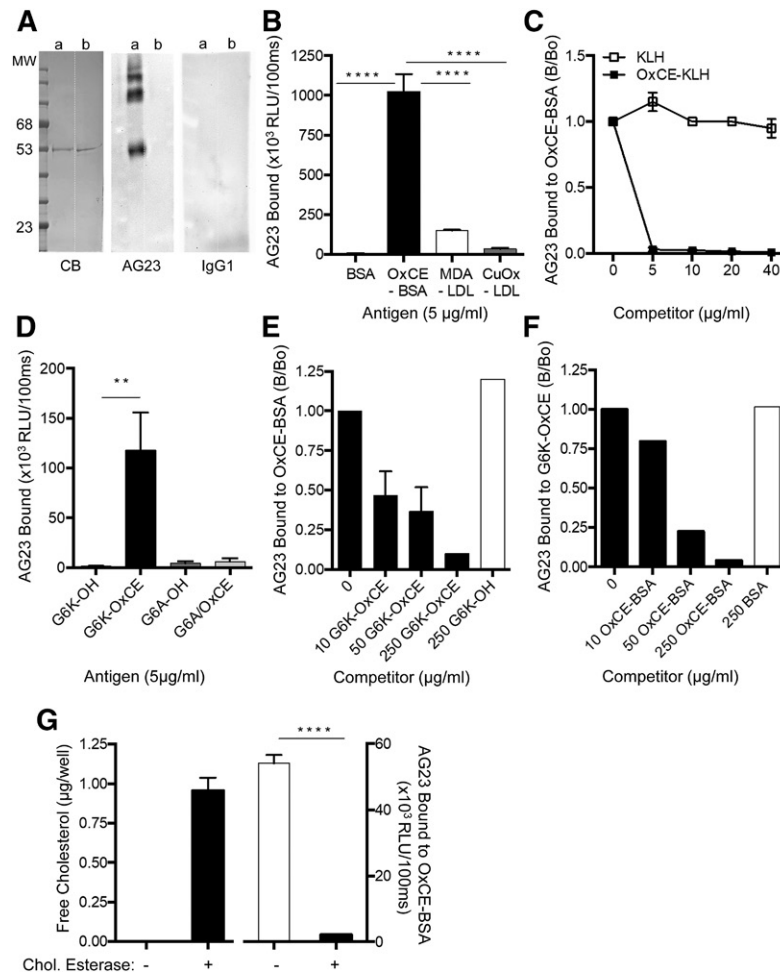


Fig. 2. AG23 specificity to OxCE epitope. A: OxCE-BSA (a) and unmodified BSA (b) were loaded on a 4–12% Bis-Tris SDS gel at 0.5 µg/well. The gel was stained with Coomassie Blue (CB) or blotted and probed with OxCE-specific AG23 mAb or a mouse anti-KLH IgG1. Representative gel and blots from 20 repeats. B: Representative results of AG23 (0.125 µg/ml) binding to BSA, OxCE-BSA, MDA-LDL, and CuOx-LDL (5 µg/ml). Four different OxCE-BSA preparations were tested in 12 independent experiments with AG23 concentrations ranging from 0.125 to 1 mg/ml. The graph shows the mean of three repeats, each in three technical replicates. Mean \pm SD; one-way ANOVA with multiple comparisons; **** P < 0.0001. C: Competition ELISA: AG23 (0.01 µg/ml) was preincubated in the absence or presence of increasing concentrations of nonmodified KLH or OxCE-KLH. Immune complexes were spun down, and supernatants were tested for binding to OxCE-BSA (5 µg/ml). Each data point is the mean of two independent assays in technical triplicates. D: AG23 (1 µg/ml) binding to 10 µg/ml of nonmodified G6K-OH and G6A-OH peptides, and the peptides subjected to the OxCE covalent modification. G6K-OxCE designates covalent modification of Lys, and G6A/OxCE designates the reaction that did not result in covalent modification of Ala. Mean \pm SD; n = 6 for G6K and n = 2 for G6A, each in technical duplicates; one-way ANOVA with multiple comparisons; ** P < 0.01. E, F: AG23 (0.15 µg/ml) was preincubated overnight with nonmodified (250 µg/ml) or OxCE-modified (10–250 µg/ml) BSA or G6K-OH peptide. Following spin down of immune complexes, supernatants were tested for binding with OxCE-BSA (E) or G6K-OxCE (F). Graphs show the results of a representative experiment performed in triplicate (E) or duplicate (F). G: OxCE plated at 1.25 µg/well in a 96-well plate was incubated with or without cholesterol esterase (10 u/well) for 3 h at 37°C. The solution was collected and pooled for free cholesterol measurements. After washes, AG23 binding to the wells was measured. Mean \pm SD, n = 5; **** P < 0.0001 (Student's t -test) for AG23 assay. Free cholesterol assay, technical triplicates of samples pooled from five wells.

i.e., levels of apoAI lipoproteins with one or more OxCE epitopes (Fig. 5C, red bars). As shown in an assay of biotinylated G6K-OxCE (supplemental Fig. S2), capture with AG23 allows for a 0.15–3.0 µM (0.01–0.2 µg/ml) linear range detection of OxCE epitopes. In a 1:50 human plasma, the upper limit of HDL particle concentration is 1.6 µM. If the assay format was flipped, and the apoAI lipoproteins were first captured on the plate and then AG23 added, the

resulting binding of AG23 was very low, below the detection limit in the majority of samples (Fig. 5C, empty bars). We did not detect OxCE associated with lipoprotein (a) [Lp(a)] (not shown).

Next, we designed an assay in which AG23 was used as a capture Ab and biotinylated AG23 was used for detection [Fig. 5A (A3)]. This format would work only if lipoproteins or other proteins carry two or more OxCE epitopes

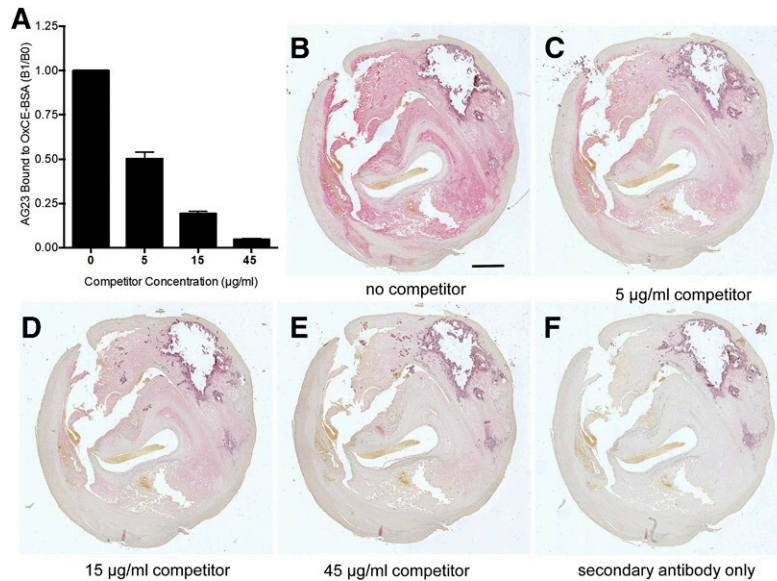


Fig. 3. AG23-specific epitopes in human atherosclerotic lesions. A: Competition of increasing concentrations of OxCE-BSA in solution for AG23 (0.1 $\mu\text{g}/\text{ml}$) binding to the plated OxCE-BSA antigen (0.5 $\mu\text{g}/\text{ml}$) was tested in an ELISA format. A representative result performed in technical triplicate. B–E: Consecutive cross-sections of human carotid endarterectomy specimens were stained with AG23 and preincubated in the absence or presence of increasing concentrations of OxCE-BSA as a competitor. F: Secondary Ab only. Representative images of three specimens tested. Scale bar, 1 mm.

accessible to AG23. The observation that low levels of binding were detected in only a few plasma samples and levels were undetectable in most (Fig. 5D) suggests that the majority of lipoproteins display only one or a few OxCE epitopes accessible to AG23.

For illustrative purposes, we combined the results of OxCE-apoB, OxCE-apoA, and “total OxCE” measurements in Fig. 5E. However, note that absolute values in these three assays cannot be compared because they use different detection Abs. Rather, Fig. 5E illustrates the limited codependence between OxCE-apoB and OxCE-apoA levels. To further analyze covariation of OxCE-apoB, OxCE-apoA, and other common lipoprotein parameters in the UVA cohort ($n = 213$) (2), we calculated Spearman correlation coefficients. As shown in **Table 1**, $r = 0.293$ between OxCE-apoB and OxCE-apoA suggests their limited covariation. OxCE-apoA did not correlate with HDL cholesterol (HDL-C). Remarkably, there was no correlation between OxPL-apoB [determined using the previously described assay (28)] and OxCE-apoB or OxCE-apoA.

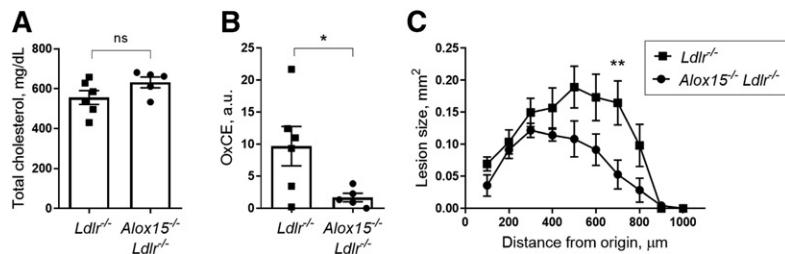


Fig. 4. AG23-specific epitopes in mouse plasma of *Ldlr*^{-/-} and *Alox15*^{-/-} *Ldlr*^{-/-} mice. A: Plasma TC from mice fed a 1% cholesterol normal fat diet for 16 weeks. B: OxCE levels were measured in mouse plasma in a sandwich ELISA using nonlabeled AG23 as a capture Ab and biotinylated AG23 as a detection Ab. C: Sections of the aortic root were collected, and lesion size was measured starting from the appearance of first leaflet in 100 μm increments. Mean \pm SEM; $n = 6$ (*Ldlr*^{-/-}) and $n = 5$ (*Alox15*^{-/-} *Ldlr*^{-/-}); * $P < 0.05$; ** $P < 0.01$. Unpaired *t*-test with Welch’s correction (A, B) and two-way ANOVA with Bonferroni posttest (C).

Effect of statin therapy on OxCE-apoB and OxCE-apoA

Next, we measured OxCE-apoB and OxCE-apoA in plasma samples from PROXI, a randomized parallel-arm double-blind placebo-controlled trial in which human subjects received placebo, 10 mg atorvastatin, 80 mg atorvastatin, or 40 mg pravastatin daily; blood was collected at baseline and after 16 weeks of treatment (16). The 40 mg pravastatin group was not analyzed in our study. At baseline, there was no difference in OxCE-apoB or OxCE-apoA levels between placebo and atorvastatin groups (not shown). After 16 weeks of treatment, OxCE-apoB levels were significantly reduced in the 10 mg and 80 mg atorvastatin groups compared with the placebo group (**Fig. 6A**). However, this covaried with the reductions in apoB-100 levels (Fig. 6B).

In contrast to reducing apoB-100, statins do not significantly change apoAI levels. Indeed, atorvastatin treatment-mediated (both 10 and 80 mg) reductions in OxCE-apoA levels (Fig. 6C) were not accompanied by changes in apoAI (Fig. 6D).

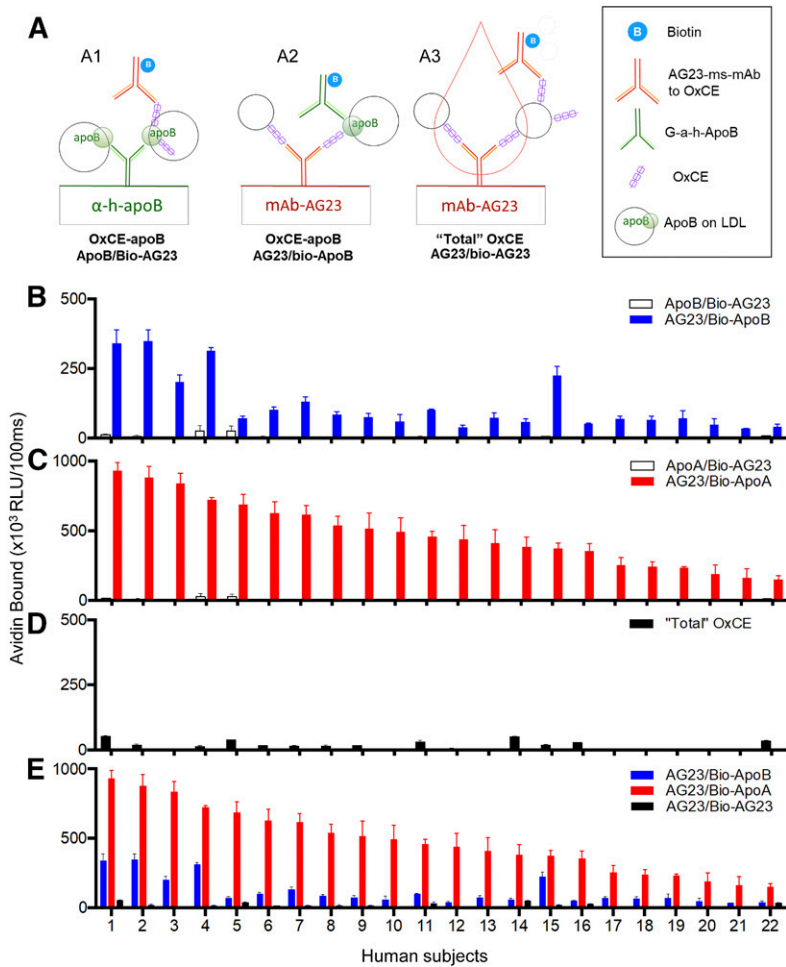


Fig. 5. Development of OxCE immunoassays. A: Schematic representation of ELISA formats for OxCE detection in human plasma. See the Materials and Methods for details. B–E: Results of different OxCE assays for 22 plasma samples from the UVA cohort representing the range of variation. Mean \pm SD of technical triplicates for each sample. Note the different scales and that absolute values cannot be compared between the assays because of use of different detection Abs.

Further, we calculated individual changes in OxCE parameters for each subject before and after treatment. As expected, atorvastatin reduced both OxCE-apoB and apoB-100 in the majority of subjects (Fig. 7A, B). However, in the absence of apoAI changes, OxCE-apoA was significantly reduced following treatment in the 80 mg atorvastatin group, but not the placebo group (Fig. 7C, D). Correlation analysis of OxCE parameters in all samples used in this study demonstrated little covariance with relevant lipoprotein measurements and, remarkably, there was no

correlation between OxPL-apoB and OxCE-apoB or OxCE-apoA (Table 2).

DISCUSSION

In this study, we have developed the mAb, AG23, that recognizes a covalent modification of proteins and peptides with OxCE. The Ab specifically stains human atherosclerotic

TABLE 1. Correlation matrix for OxCE-apoB and OxCE-apoA versus OxPL-apoB and common lipoprotein biomarkers in UVA cohort

	OxCE-apoB	OxCE-apoA	TC	LDL-C	HDL-C	TG	OxPL-apoB
OxCE-apoB	—	0.293 (<0.0001)	0.357 (<0.0001)	0.231 (<0.001)	0.031 (n.s.)	0.460 (<0.0001)	-0.029 (n.s.)
OxCE-apoA	0.293 (<0.0001)	—	0.445 (<0.0001)	0.422 (<0.0001)	-0.027 (n.s.)	0.193 (<0.005)	-0.043 (n.s.)
TC	0.357 (<0.0001)	0.445 (<0.0001)	—	0.942 (<0.0001)	0.369 (<0.0001)	0.292 (<0.0001)	-0.054 (n.s.)
LDL-C	0.231 (<0.001)	0.422 (<0.0001)	0.942 (<0.0001)	—	0.276 (<0.0001)	0.166 (<0.05)	-0.092 (n.s.)
HDL-C	0.031 (n.s.)	-0.027 (n.s.)	0.369 (<0.0001)	0.276 (<0.0001)	—	-0.443 (<0.0001)	-0.022 (n.s.)
TG	0.460 (<0.0001)	0.193 (<0.005)	0.292 (<0.0001)	0.166 (<0.05)	-0.443 (<0.0001)	—	0.089 (n.s.)
OxPL-apoB	-0.029 (n.s.)	-0.043 (n.s.)	-0.054 (n.s.)	-0.092 (n.s.)	-0.022 (n.s.)	0.089 (n.s.)	—

Correlation coefficient (P). Nonparametric Spearman test; $n = 213$. TG, triglycerides; n.s., nonsignificant.

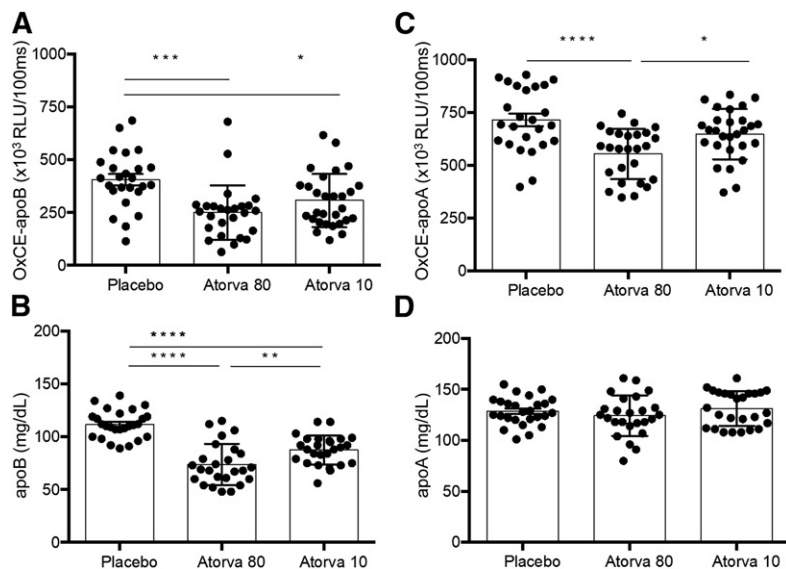


Fig. 6. Effect of atorvastatin versus placebo treatment on OxCE-apoB and OxCE-apoA levels. Plasma samples collected from subjects after a 16 week treatment with placebo (n = 25) or atorvastatin (Atorva) 80 mg (n = 26) or 10 mg (n = 29) were tested for OxCE-apoB (A) and OxCE-apoA (C). The plasma apoB (B) and apoA (D) levels are from the original PROXI study as reported. Each data point is the mean of three technical replicates. Mean \pm SEM, one-way ANOVA with multiple comparisons; * $P < 0.05$; ** $P < 0.01$; *** $P < 0.001$; **** $P < 0.0001$.

lesions and enables detection of OxCE epitopes in human plasma. The ELISA assay that we have developed measures levels of lipoproteins that have one or more OxCE epitopes, but it does not measure the levels of OxCE per lipoprotein. However, results of a “total OxCE” immunoassay, with AG23 serving as both capture and detection Ab, show detectable but low signals in only a few samples, suggesting that lipoproteins and other components of plasma rarely have more than one AG23-accessible OxCE epitope. This is in contrast to the well-characterized OxPL-apoB assay, demonstrating consistently robust signals across multiple human cohorts (28–31). Among all apoB lipoproteins, OxPL is predominantly found in Lp(a), and the levels of OxPL-apoB and Lp(a) strongly correlate (32).

Another remarkable difference between OxPL and OxCE biomarkers is that the levels of OxPL associated with apoAI lipoproteins are low (33), whereas OxCE was readily detected in apoAI lipoproteins in all the human plasma samples that we tested. These results suggest that OxCE-apoA can be a useful independent biomarker, complementing the

information obtained with OxPL-apoB. Indeed, there was no correlation between OxCE-apoA and OxPL-apoB or apoAI or HDL-C levels. Atorvastatin treatment reduced OxCE-apoA levels, and OxCE-apoA levels were independent of the levels of apoAI. Future outcome studies will determine whether OxCE-apoA and/or OxCE-apoB have any prognostic value.

Oxidation of cholesteryl arachidonate with a lipophilic free radical initiator, the reaction used in preparation of OxCE, results in oxygenation of the CE acyl chain (2, 12, 34). The chemistry of this reaction is well-described; it produces polyoxygenated OxCE, including formation of bicyclic endoperoxide and hydroperoxide groups in the acyl chain, and can be initiated by the presence of 15(*S*)-hydroperoxyeicosatetraenoic acid (34–36). The latter is a product of 12/15LO enzymatic activity, which is considered a major factor in LDL oxidation in vivo (15, 24). Hypercholesterolemic *Alox15*^{-/-} mice develop less atherosclerosis than the mice with functional 12/15LO (37, 38) and, as we show in this work, have lower plasma levels

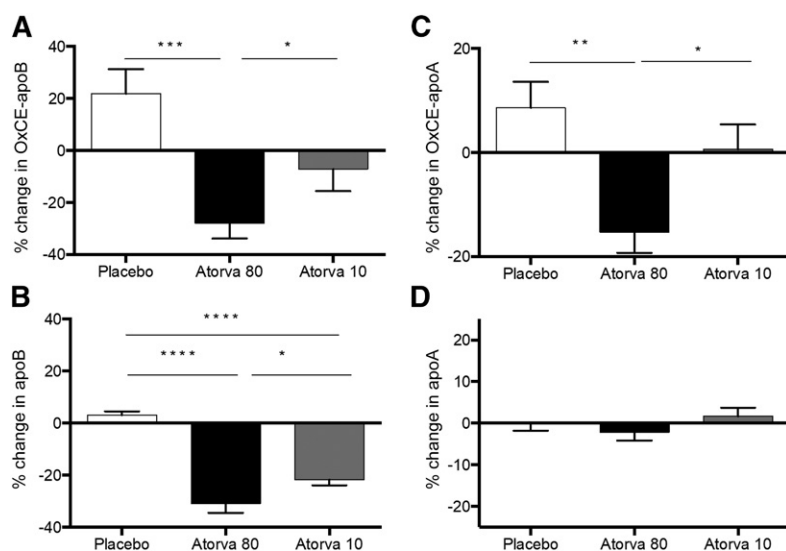


Fig. 7. Changes in OxCE-apoB and OxCE-apoA parameters from baseline to posttreatment with atorvastatin versus placebo. Individual changes from baseline to posttreatment were calculated for OxCE-apoB (A), apoB (B), OxCE-apoA (C), and apoA (D). Placebo (n = 24), atorvastatin (Atorva) 80 mg (n = 25) or 10 mg (n = 25) groups. Differences in subject numbers between Figs. 5 and 6 are due to missing baseline samples. Mean \pm SEM, one-way ANOVA with multiple comparisons; * $P < 0.05$; ** $P < 0.01$; *** $P < 0.001$; **** $P < 0.0001$.

TABLE 2. Correlation matrix for OxCE-apoB and OxCE-apoA versus OxPL-apoB and common lipoprotein biomarkers in PROXI cohorts


	OxCE-apoB	OxCE-apoA	TC	LDL-C	HDL-C	apoB-100	apoAI	TG	OxPL-apoB
OxCE-apoB	—	0.426 (<0.0001)	0.379 (<0.0001)	0.413 (<0.0001)	-0.169 (<0.05)	0.427 (<0.0001)	-0.085 (n.s.)	0.179 (<0.05)	0.003 (n.s.)
OxCE-apoA	0.426 (<0.0001)	—	0.362 (<0.0001)	0.216 (<0.01)	0.050 (n.s.)	0.211 (<0.01)	0.152 (n.s.)	0.344 (<0.0001)	0.008 (n.s.)
TC	0.379 (<0.0001)	0.362 (<0.0001)	—	0.947 (<0.0001)	-0.051 (n.s.)	0.830 (<0.0001)	0.068 (n.s.)	0.454 (<0.0001)	-0.074 (n.s.)
LDL-C	0.413 (<0.0001)	0.216 (<0.01)	0.947 (<0.0001)	—	-0.118 (n.s.)	0.853 (<0.0001)	-0.047 (n.s.)	0.272 (<0.0001)	-0.039 (n.s.)
HDL-C	-0.169 (<0.05)	0.050 (n.s.)	-0.051 (n.s.)	-0.118 (n.s.)	—	-0.272 (<0.001)	0.828 (<0.0001)	-0.448 (<0.0001)	0.060 (n.s.)
apoB-100	0.427 (<0.0001)	0.211 (<0.01)	0.830 (<0.0001)	0.853 (<0.0001)	-0.272 (<0.001)	—	-0.097 (n.s.)	0.447 (<0.0001)	-0.044 (n.s.)
apoAI	-0.085 (n.s.)	0.152 (n.s.)	0.068 (n.s.)	-0.047 (n.s.)	0.828 (<0.0001)	-0.097 (n.s.)	—	-0.147 (n.s.)	0.069 (n.s.)
TG	0.179 (<0.05)	0.344 (<0.0001)	0.454 (<0.0001)	0.272 (<0.001)	-0.448 (<0.0001)	0.447 (<0.0001)	-0.147 (n.s.)	—	-0.108 (n.s.)
OxPL-apoB	0.003 (n.s.)	0.008 (n.s.)	-0.074 (n.s.)	-0.039 (n.s.)	0.060 (n.s.)	-0.044 (n.s.)	0.07 (n.s.)	-0.108 (n.s.)	—

Correlation coefficient (*P*). Both baseline and posttreatment samples (*n* = 160) were analyzed by nonparametric Spearman test. TG, triglyceride; n.s., nonsignificant.

of AG23-reactive OxCE epitopes. Because the presence of bicyclic endoperoxide and hydroperoxide products on the acyl chain characterize early stages of LDL oxidation, it was not surprising to detect low levels of AG23-reactive epitopes in MDA-LDL, subjected during preparation to prolonged incubation and dialysis steps, but not in CuOxLDL in which Cu²⁺-mediated, extensive lipid oxidation is characterized by formation of truncated fatty acyl aldehydes and oxysterols. Because OxCE contains bicyclic endoperoxides (2), it can conjugate to NH₂ groups, such as lysine. Under protic conditions, e.g., when accessible to protein nucleophiles, bicyclic endoperoxides open to form highly reactive isolevuglandins (also known as isoketals), which readily form covalent adducts with proteins (39–41).

Yet, the limitation of this study is in an incomplete characterization of the OxCE epitope recognized by AG23. We used an unseparated reaction product of cholesteryl arachidonate oxidation with a lipophilic free radical initiator to modify BSA, KLH, and G6K. The result that cholesterol esterase treatment abolishes AG23 binding to OxCE-BSA suggests the preservation of cholesteryl (or its part) in the OxCE epitope recognized by AG23, or that it is required for the correct configuration of the AG23 epitope to be recognized. However, more detailed characterization of the epitope is complicated by differences in the mass spectrometry strategies utilized to analyze proteins and lipids. We also do not know whether oxidized cholesteryl linoleate covalent modification of a protein would be recognized by AG23. An Ab to the oxidized cholesteryl linoleate-protein conjugates has been reported to detect epitopes in atherosclerotic lesions (14), and oxidized cholesteryl linoleate is a predominant OxCE found in human lesions (3, 11). AG23 is likely different from reported Abs to unesterified cholesterol, as the majority of those were obtained by immunizing animals with cholesterol crystals or cholesterol-rich liposomes (42). In addition to a different geometry of the unesterified cholesterol molecule in crystals or in the

lipid bilayer from that of OxCE-protein conjugates, immunogenicity of unesterified cholesterol was in large part determined by the 3β-hydroxyl group (42), absent in CE. Our findings that polyoxygenated cholesteryl arachidonate hydroperoxides activate TLR4 and induce inflammatory responses in macrophages (2) guided our strategy to develop an Ab to biologically active proinflammatory adducts of oxidized cholesteryl arachidonate to proteins.

In summary, we developed a new OSE Ab, which recognizes OxCE epitopes on lipoproteins, and potential new biomarker assays for measuring OxCE in apoB-100 and apoAI lipoproteins. Future studies will determine whether OxCE-related measures will predict CVD events and provide enhanced risk discrimination in addition to currently measured clinical variables. 

REFERENCES

- Miller, Y. I., S-H. Choi, P. Wiesner, L. Fang, R. Harkewicz, K. Hartvigsen, A. Boullier, A. Gonen, C. J. Diehl, X. Que, et al. 2011. Oxidation-specific epitopes are danger associated molecular patterns recognized by pattern recognition receptors of innate immunity. *Circ. Res.* **108**: 235–248.
- Choi, S-H., H. Yin, A. Ravandi, A. Armando, D. Dumlaio, J. Kim, F. Almazan, A. M. Taylor, C. A. McNamara, S. Tsimikas, et al. 2013. Polyoxygenated cholesterol ester hydroperoxide activates TLR4 and SYK dependent signaling in macrophages. *PLoS One.* **8**: e83145.
- Ravandi, A., G. Leibundgut, M. Y. Hung, M. Patel, P. M. Hutchins, R. C. Murphy, A. Prasad, E. Mahmud, Y. I. Miller, E. A. Dennis, et al. 2014. Release and capture of bioactive oxidized phospholipids and oxidized cholesteryl esters during percutaneous coronary and peripheral arterial interventions in humans. *J. Am. Coll. Cardiol.* **63**: 1961–1971.
- Choi, S. H., D. Sviridov, and Y. I. Miller. 2017. Oxidized cholesteryl esters and inflammation. *Biochim. Biophys. Acta Mol. Cell Biol. Lipids.* **1862**: 393–397.
- Choi, S. H., J. Kim, A. Gonen, S. Viriyakosol, and Y. I. Miller. 2016. MD-2 binds cholesterol. *Biochem. Biophys. Res. Commun.* **470**: 877–880.
- Gruber, A., M. Mancek, H. Wagner, C. J. Kirschning, and R. Jerala. 2004. Structural model of MD-2 and functional role of its basic amino acid clusters involved in cellular lipopolysaccharide recognition. *J. Biol. Chem.* **279**: 28475–28482.

7. Folcik, V. A., and M. K. Cathcart. 1994. Predominance of esterified hydroperoxy-linoleic acid in human monocyte-oxidized LDL. *J. Lipid Res.* **35**: 1570–1582.
8. Hoppe, G., A. Ravandi, D. Herrera, A. Kuksis, and H. F. Hoff. 1997. Oxidation products of cholesteryl linoleate are resistant to hydrolysis in macrophages, form complexes with proteins, and are present in human atherosclerotic lesions. *J. Lipid Res.* **38**: 1347–1360.
9. Suarna, C., R. T. Dean, J. May, and R. Stocker. 1995. Human atherosclerotic plaque contains both oxidized lipids and relatively large amounts of α -tocopherol and ascorbate. *Arterioscler. Thromb. Vasc. Biol.* **15**: 1616–1624.
10. Upston, J. M., X. Niu, A. J. Brown, R. Mashima, H. Wang, R. Senthilmohan, A. J. Kettle, R. T. Dean, and R. Stocker. 2002. Disease stage-dependent accumulation of lipid and protein oxidation products in human atherosclerosis. *Am. J. Pathol.* **160**: 701–710.
11. Hutchins, P. M., E. E. Moore, and R. C. Murphy. 2011. Electrospray tandem mass spectrometry reveals extensive and non-specific oxidation of cholesterol esters in human peripheral vascular lesions. *J. Lipid Res.* **52**: 2070–2083.
12. Harkewicz, R., K. Hartvigsen, F. Almazan, E. A. Dennis, J. L. Witztum, and Y. I. Miller. 2008. Cholesteryl ester hydroperoxides are biologically active components of minimally oxidized LDL. *J. Biol. Chem.* **283**: 10241–10251.
13. Fang, L., R. Harkewicz, K. Hartvigsen, P. Wiesner, S. H. Choi, F. Almazan, J. Pattison, E. Deer, T. Sayaphupha, E. A. Dennis, et al. 2010. Oxidized cholesteryl esters and phospholipids in zebrafish larvae fed a high-cholesterol diet: macrophage binding and activation. *J. Biol. Chem.* **285**: 32343–32351.
14. Kawai, Y., A. Saito, N. Shibata, M. Kobayashi, S. Yamada, T. Osawa, and K. Uchida. 2003. Covalent binding of oxidized cholesteryl esters to protein: implications for oxidative modification of low density lipoprotein and atherosclerosis. *J. Biol. Chem.* **278**: 21040–21049.
15. Miller, Y. I., and J. Y. Shyy. 2017. Context-dependent role of oxidized lipids and lipoproteins in inflammation. *Trends Endocrinol. Metab.* **28**: 143–152.
16. Ky, B., A. Burke, S. Tsimikas, M. L. Wolfe, M. G. Tadesse, P. O. Szapary, J. L. Witztum, G. A. FitzGerald, and D. J. Rader. 2008. The influence of pravastatin and atorvastatin on markers of oxidative stress in hypercholesterolemic humans. *J. Am. Coll. Cardiol.* **51**: 1653–1662.
17. Gonen, A., L. F. Hansen, W. W. Turner, E. N. Montano, X. Que, A. Rafia, M. Y. Chou, P. Wiesner, D. Tsiantoulas, M. Corr, et al. 2014. Atheroprotective immunization with malondialdehyde-modified LDL is hapten specific and dependent on advanced MDA adducts: implications for development of an atheroprotective vaccine. *J. Lipid Res.* **55**: 2137–2155.
18. Palinski, W., S. Horkko, E. Miller, U. P. Steinbrecher, H. C. Powell, L. K. Curtiss, and J. L. Witztum. 1996. Cloning of monoclonal auto-antibodies to epitopes of oxidized lipoproteins from apolipoprotein E-deficient mice. Demonstration of epitopes of oxidized low density lipoprotein in human plasma. *J. Clin. Invest.* **98**: 800–814.
19. Sun, D., and C. D. Funk. 1996. Disruption of 12/15-lipoxygenase expression in peritoneal macrophages. Enhanced utilization of the 5-lipoxygenase pathway and diminished oxidation of low density lipoprotein. *J. Biol. Chem.* **271**: 24055–24062.
20. Tsimikas, S., A. Miyanojima, K. Hartvigsen, E. Merki, P. X. Shaw, M. Y. Chou, J. Pattison, M. Torzewski, J. Sollors, T. Friedmann, et al. 2011. Human oxidation-specific antibodies reduce foam cell formation and atherosclerosis progression. *J. Am. Coll. Cardiol.* **58**: 1715–1727.
21. Choi, S. H., P. Wiesner, F. Almazan, J. Kim, and Y. I. Miller. 2012. Spleen tyrosine kinase regulates AP-1 dependent transcriptional response to minimally oxidized LDL. *PLoS One.* **7**: e32378.
22. Young, S. G., J. L. Witztum, D. C. Casal, L. K. Curtiss, and S. Bernstein. 1986. Conservation of the low density lipoprotein receptor-binding domain of apoprotein B. Demonstration by a new monoclonal antibody, MB47. *Arteriosclerosis.* **6**: 178–188.
23. Funk, C. D., and T. Cyrus. 2001. 12/15-Lipoxygenase, oxidative modification of LDL and atherogenesis. *Trends Cardiovasc. Med.* **11**: 116–124.
24. Zhao, L., and C. D. Funk. 2004. Lipoxygenase pathways in atherogenesis. *Trends Cardiovasc. Med.* **14**: 191–195.
25. Belkner, J., H. Stender, and H. Kuhn. 1998. The rabbit 15-lipoxygenase preferentially oxygenates LDL cholesterol esters, and this reaction does not require vitamin E. *J. Biol. Chem.* **273**: 23225–23232.
26. Hutchins, P. M., and R. C. Murphy. 2012. Cholesteryl ester acyl oxidation and remodeling in murine macrophages: formation of oxidized phosphatidylcholine. *J. Lipid Res.* **53**: 1588–1597.
27. George, J., A. Afek, A. Shaish, H. Levkovitz, N. Bloom, T. Cyrus, L. Zhao, C. D. Funk, E. Sigal, and D. Harats. 2001. 12/15-Lipoxygenase gene disruption attenuates atherogenesis in LDL receptor-deficient mice. *Circulation.* **104**: 1646–1650.
28. Taleb, A., J. L. Witztum, and S. Tsimikas. 2011. Oxidized phospholipids on apoB-100-containing lipoproteins: a biomarker predicting cardiovascular disease and cardiovascular events. *Biomark. Med.* **5**: 673–694.
29. Byun, Y. S., J. H. Lee, B. J. Arsenault, X. Yang, W. Bao, D. DeMicco, R. Laskey, J. L. Witztum, and S. Tsimikas. 2015. Relationship of oxidized phospholipids on apolipoprotein B-100 to cardiovascular outcomes in patients treated with intensive versus moderate atorvastatin therapy: the TNT trial. *J. Am. Coll. Cardiol.* **65**: 1286–1295.
30. Tsimikas, S., P. Willeit, J. Willeit, P. Santer, M. Mayr, Q. Xu, A. Mayr, J. L. Witztum, and S. Kiechl. 2012. Oxidation-specific biomarkers, prospective 15-year cardiovascular and stroke outcomes, and net reclassification of cardiovascular events. *J. Am. Coll. Cardiol.* **60**: 2218–2229.
31. Byun, Y. S., X. Yang, W. Bao, D. DeMicco, R. Laskey, J. L. Witztum, and S. Tsimikas. 2017. Oxidized phospholipids on apolipoprotein B-100 and recurrent ischemic events following stroke or transient ischemic attack. *J. Am. Coll. Cardiol.* **69**: 147–158.
32. Bergmark, C., A. Dewan, A. Orsoni, E. Merki, E. R. Miller, M. J. Shin, C. J. Binder, S. Horkko, R. M. Krauss, M. J. Chapman, et al. 2008. A novel function of lipoprotein [a] as a preferential carrier of oxidized phospholipids in human plasma. *J. Lipid Res.* **49**: 2230–2239.
33. Arai, K., A. Orsoni, Z. Mallat, A. Tedgui, J. L. Witztum, E. Bruckert, A. D. Tselepis, M. J. Chapman, and S. Tsimikas. 2012. Acute impact of apheresis on oxidized phospholipids in patients with familial hypercholesterolemia. *J. Lipid Res.* **53**: 1670–1678.
34. Yin, H., J. D. Morrow, and N. A. Porter. 2004. Identification of a novel class of endoperoxides from arachidonate autoxidation. *J. Biol. Chem.* **279**: 3766–3776.
35. Yin, H., C. M. Havrilla, J. D. Morrow, and N. A. Porter. 2002. Formation of isoprostane bicyclic endoperoxides from the autoxidation of cholesteryl arachidonate. *J. Am. Chem. Soc.* **124**: 7745–7754.
36. Yin, H., C. M. Havrilla, L. Gao, J. D. Morrow, and N. A. Porter. 2003. Mechanisms for the formation of isoprostane endoperoxides from arachidonic acid. “Dioxetane” intermediate versus beta-fragmentation of peroxy radicals. *J. Biol. Chem.* **278**: 16720–16725.
37. Cyrus, T., J. L. Witztum, D. J. Rader, R. Tangirala, S. Fazio, M. F. Linton, and C. D. Funk. 1999. Disruption of the 12/15-lipoxygenase gene diminishes atherosclerosis in apo E-deficient mice. *J. Clin. Invest.* **103**: 1597–1604.
38. Cyrus, T., D. Pratico, L. Zhao, J. L. Witztum, D. J. Rader, J. Rokach, G. A. FitzGerald, and C. D. Funk. 2001. Absence of 12/15-lipoxygenase expression decreases lipid peroxidation and atherogenesis in apolipoprotein e-deficient mice. *Circulation.* **103**: 2277–2282.
39. Salomon, R. G., K. Kaur, and E. Batyeva. 2000. Isoeuglandin-protein adducts in oxidized low density lipoprotein and human plasma: a strong connection with cardiovascular disease. *Trends Cardiovasc. Med.* **10**: 53–59.
40. Salomon, R. G. 2005. Isoeuglandins, oxidatively truncated phospholipids, and atherosclerosis. *Ann. N. Y. Acad. Sci.* **1043**: 327–342.
41. Li, W., J. M. Laird, L. Lu, S. Roychowdhury, L. E. Nagy, R. Zhou, J. W. Crabb, and R. G. Salomon. 2009. Isoeuglandins covalently modify phosphatidylethanolamines in vivo: detection and quantitative analysis of hydroxylactam adducts. *Free Radic. Biol. Med.* **47**: 1539–1552.
42. Ohno-Iwashita, Y., Y. Shimada, M. Hayashi, M. Iwamoto, S. Iwashita, and M. Inomata. 2010. Cholesterol-binding toxins and anti-cholesterol antibodies as structural probes for cholesterol localization. *Subcell. Biochem.* **51**: 597–621.